Nano-Structures & Nano-Objects 29 (2022) 100810

Contents lists available at ScienceDirect

Nano-Structures & Nano-Objects

journal homepage: www.elsevier.com/locate/nanoso

Green synthesis of an Ag nanoparticle-decorated graphene nanoplatelet nanocomposite by using *Cleistocalyx operculatus* leaf extract for antibacterial applications

Hong Phuong Nguyen Thi [a], Kieu Trang Pham Thi [a,b], Le Nguyen Thi [a], Thanh Tung Nguyen [c], Phuong T.M. Nguyen [d,e], Tri Thien Vu [f], Hau Thi Le [a], Trung-Dung Dang [a,*], Dang Chinh Huynh [a], Huu Thuan Mai [g], Duc Duong La [f,*], S. Wong Chang [i], D. Duc Nguyen [h,i,*]

[a] *School of Chemical Engineering, Hanoi University of Science and Technology, 1 Dai Co Viet, Hanoi, Vietnam*
[b] *Applied Nanotechnology Joint-stock company, Tay Ho, Hanoi, Vietnam*
[c] *Institute of Materials Science, Vietnam Academy of Science and Technology, 18-Hoang Quoc Viet, Hanoi, Vietnam*
[d] *Institute of Graduate University of Science and Technology, Vietnam Academy of Science and Technology, Hanoi, Vietnam*
[e] *Institute of Biotechnology, Vietnam Academy of Science and Technology, Hanoi, Vietnam*
[f] *Institute of Chemistry and Materials, Nghia Do, Cau Giay, Hanoi, Vietnam*
[g] *School of Engineering Physics, Hanoi University of Science and Technology, 1 Dai Co Viet, Hanoi, Vietnam*
[h] *Faculty of Environmental and Food Engineering, Nguyen Tat Thanh University, 300A Nguyen Tat Thanh, District 4, Ho Chi Minh City, 755414, Vietnam*
[i] *Department of Environmental Energy Engineering, Kyonggi University, Suwon-si 16227, Republic of Korea*

ARTICLE INFO

Article history:
Received 20 July 2021
Received in revised form 6 October 2021
Accepted 26 October 2021

Keywords:
Green synthesis
Cleistocalyx operculatus extract
Ag nanoparticle/graphene nanoplatelet nanocomposite
Antibacterial activity

ABSTRACT

In the past few years, green synthesis has been extensively utilized as an environmentally friendly and affordable approach for the preparation of nanomaterials. Many extracts from plants have been employed as green reductants for these syntheses. For the first time, the *Cleistocalyx operculatus* leaf extract was employed as a green reductant to synthesize Ag nanoparticles decorated on the surfaces of graphene nanoplatelets. Moreover, the behavior of the components in the extract on the formation of the Ag nanoparticles is discussed herein. The prepared Ag nanoparticle/graphene nanoplatelet nanocomposite was characterized using X-ray diffraction, scanning electron microscopy, energy dispersive spectroscopy and mapping, and Fourier-transform infrared spectroscopy. The results show that the Ag nanoparticles were 20–40 nm in diameter and were uniformly distributed on the surface of the graphene nanoplatelets. In addition, the green-synthesized Ag nanoparticle/graphene nanoplatelet nanocomposite also demonstrated excellent antibacterial activity toward *Escherichia coli*, thereby showing its promise for use as a disinfectant.

1. Introduction

Nanomaterials have been extensively studied and their applicability in many research fields and industrial processes has been widely reported [1–4]. Ag nanoparticles, with excellent optical and biological properties, have been widely researched and utilized in many research fields and medical processes, including (but not limited to) as an antimicrobial agent and in medical devices, sensors and drug delivery systems [5–7]. In comparison to the bulk form, Ag nanoparticles have outstanding optical, mechanical, catalytic, thermal and electronic properties that strongly depend on the synthesis approach for the size, and morphology of the Ag crystals. However, Ag^+ ions are easily released by Ag nanostructures and are cytotoxic [8], which limits the use of Ag nanoparticles in bioapplications [9]. Thus, modification of Ag nanoparticles with other materials, such as graphene, carbon nanotubes, activated carbon and aerogel significantly improves the stability and activity of the Ag nanoparticles [4,10–12]. This combination also reveals enhanced antimicrobial efficiency in comparison to free-standing Ag nanoparticles [13,14].

Graphene is a two-dimensional (2D) material with remarkable physical, chemical and electrical properties that has attracted extensive attention from scientists worldwide [15–17]. It has been widely employed in many applications, such as environmental remediation, sensors, functional painting, energy storage, smart textiles and composites [7,18–22]. Most recently, graphene

* Corresponding authors.
E-mail addresses: dung.dangtrung@hust.edu.vn (T.-D. Dang), duc.duong.la@gmail.com (D.D. La), nguyensyduc@gmail.com (D.D. Nguyen).

https://doi.org/10.1016/j.nanoso.2021.100810
2352-507X/

has been employed as a substrate to improve the antimicrobial activity of many nanomaterials based on Ag, ZnO, TiO_2 and Cu because of its high surface area and flexibility [23,24]. Among these, many researchers have focused on graphene-supported Ag nanoparticles due to their excellent optical, electronic, catalytic and antibacterial properties [14,25–27]. It has been demonstrated that graphene is an effective substrate for distributing and preventing the aggregation of Ag nanoparticles. Many approaches have been utilized in the formation of Ag nanoparticle/graphene nanoplatelet nanocomposites, such as chemical [28,29], biological [30] and microwave irradiation [28]. Among these, the chemical approach extensively employed different reducing agents with high reducing activity, such as sodium borohydride ($NaBH_4$) [28,31], sodium citrate [32] and ascorbic acid [33]. However, these chemicals are expensive, as well as toxic to the environment and human health. Thus, alternative methods to effectively and safely synthesize graphene@Ag nanocomposites are urgently required. Because of these reasons, green synthesis, which uses nature-derived reductants instead of chemical reducing agents, has attracted enormous attention [10,34–39]. Many research groups have successfully fabricated Ag nanoparticles of 20−100 nm in size from plant extracts such as mulberry leaves [40], latex from *Jatropha curcas* [41], *Terminalia catappa* leaves [42]. Chandu, Chittajallu, Mukkavilli, Pilli and Bollikolla [15] successfully fabricated an Ag nanoparticle-decorated reduced graphene oxide (rGO) nanocomposite by using a custard apple leaf extract that exhibited remarkable photocatalytic activity toward methylene blue under sunlight irradiation. In another study, Chettri et al. [43] employed *Psidium guajava* extract to simultaneously reduce Ag ions and rGO to fabricate an Ag nanoparticle/rGO nanocomposite and evaluate its use in the surface-enhanced Raman spectroscopy detection of methylene blue.

Cleistocalyx operculatus is a tropical plant that is widely distributed in many places in Asia, such as China, Laos, Cambodia and Vietnam. The leaves and flower buds of *C. operculatus* have been utilized for medical applications to improve digestion, as an antibacterial agent and so on. The leaf extract composition of *C. operculatus* consists of polyphenols, flavonoids, vitamins and minerals, and thus the leaves have an acrid and mildly bitter taste. The high polyphenol content in the *C. operculatus* leaf extract can be effectively used as a green reductant to synthesize nanomaterials. Furthermore, other components in the extract can be used as a functional coating to prevent the metals in nanoscale structures from oxidizing. However, the use of the *C. operculatus* extract for the green synthesis of nanomaterials has not previously been investigated.

In the present study, an Ag nanoparticle-decorated graphene nanoplatelet nanocomposite was facilely fabricated by using *C. operculatus* leaf extract as a green reductant and stabilizing agent for the first time. Moreover, its antibacterial properties and stability are compared with free-standing Ag nanoparticles.

2. Experimental section

2.1. Materials

C. operculatus leaves were collected, dried and ground into a powder. The extraction procedure was adapted from a previous work [44]. Typically, 5 g of the dried powder was boiled and constantly stirred in 30 mL of ethanol at 50–60 °C for 2 h. The polyphenol and flavonoid amounts in the resulting *C. operculatus* leaf extract were determined as 12.5% and 0.62%, respectively, as determined according to the protocols in [45,46]. For reducing purposes, concentrated *C. operculatus* leaf extract was diluted 20 times with deionized water.

A well-dispersed graphene aqueous solution (10 g/L) was obtained from Applied Nanotechnology Jsc. Silver nitrate ($AgNO_3$) and ethanol were obtained from Sigma Aldrich. All chemicals were used as received without any further purification.

2.2. Synthesis of the Ag nanoparticle/graphene nanoplatelet nanocomposite

Various amounts of $AgNO_3$ were dissolved in 15 mL of deionized water containing graphene nanoplatelets (10 g/L) by ultrasonic stirring for around 15 min, resulting in various graphene/Ag^+ ratios (30% (2.5 g/L Ag^+), 50% (4.18 g/L Ag^+), 70% (5.8 g/L Ag^+) and 100% (8.3 g/L Ag^+)). 30 mL of diluted *C. operculatus* extract was added dropwise to the $AgNO_3$/graphene solution under ambient conditions. The mixture was stirred during the diluted extract addition and for 15 min thereafter. Next, the Ag nanoparticle/graphene nanoplatelet nanocomposite was centrifuged and washed with ethanol, followed by five times with distilled water. The resulting nanocomposite was dried at 60 °C and stored before further use. For comparison, the Ag nanoparticles were prepared by using the same procedure, but without the presence of graphene.

2.3. Characterization

The prepared Ag nanoparticle/graphene nanoplatelet nanocomposite morphology and element distribution were observed using an energy dispersive X-ray (EDX)-equipped scanning electron microscope (SEM, Hitachi S-4600, Japan). Fourier-transform infrared (FTIR) spectroscopy (TENSOR II, Bruker Co., Germany) was employed to identify any functional groups on the surface of the Ag nanoparticle/graphene nanoplatelet nanocomposite. The crystallinity of the nanocomposite was examined by X-ray diffraction (XRD, X'Pert PRO PANalytical PW3040/60, Malvern Panalytical Co., the Netherlands) with a 0.15405 nm Cu-Kα radiation source.

2.4. Measurement of the antibacterial activity of the Ag nanoparticle/graphene nanoplatelet nanocomposites

Compositions of Luria Bertani (LB) broth and LB agar environments containing 10 g tryptone, 5 g yeast extract power, 5 g sodium chloride (NaCl), and 15 g agar in 1 L distilled water were prepared in advance of the experiments. The antimicrobial activities of the Ag nanoparticle/graphene nanoplatelet nanocomposites were assessed against *Escherichia coli* by the agar disk diffusion method. Bacterial colonies of *E. coli* from the original strain were grown in an LB agar environment. After colony formation, 5 mL of them were transferred to LB broth and shaken at 37 °C overnight. Various volumes (50, 100 and 200 μL) of 0.1% Ag nanoparticle/graphene nanoplatelet nanocomposite solution were added to the agar wells on the petri dish and the test plates were incubated at 4–10 °C for 2 h so that the wells diffused into the bacterial culture environment. Subsequently, the dishes were put into an incubator at 37 °C for 24 h. The positive control was 5 mg/mL solution of a kanamycin antibiotic solution and the negative control was sterile distilled water.

3. Results and discussion

It is well-known that the polyphenol and flavonoid content in leaf extracts can be used to reduce Ag^+ ions to produce Ag nanoparticles [47,48]. Thus, it is necessary to determine the amounts of these in each extract to evaluate the potential of the reducing performance. The polyphenol and flavonoid amounts in the *C. operculatus* extract were determined as 12.4 and 0.62%,

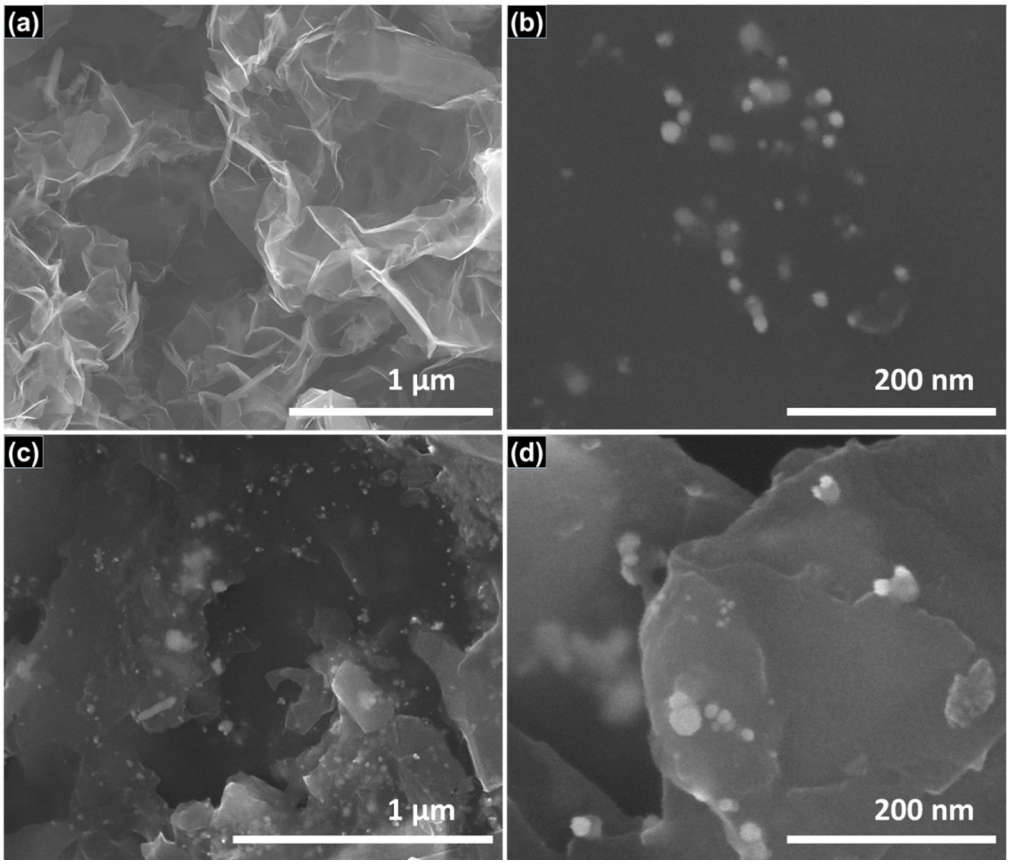

Fig. 1. SEM images of (a) graphene, (b) Ag nanoparticles and (c,d) the Ag nanoparticle/graphene nanoplatelet nanocomposite prepared by a green synthesis with an Ag nanoparticle/graphene nanoplatelet mass ratio of 1:1 (100% Ag).

respectively, which are relatively high compared to other plant extracts.

The surface morphologies of the graphene nanoplatelets, Ag nanoparticles and Ag nanoparticle/graphene nanoplatelet nanocomposite were observed in the SEM images shown in Fig. 1. The morphology of the graphene was crumpled, wrinkled and semi-transparent in the electron beam of the SEM instrument, demonstrating that the graphene consists of a few layers (Fig. 1a) [39,49]. The SEM image in Fig. 1b indicates that Ag nanoparticles with an average diameter of approximately 20 nm were successfully fabricated using the *C. operculatus* extract. SEM images of Ag nanoparticle/graphene nanoplatelet nanocomposites prepared with various Ag loading amounts are shown in Figure S1; slight differences in the morphologies of the resulting nanocomposites can be observed, with the one obtained with an Ag loading of 100% exhibiting the highest density and most regular size of the Ag nanoparticles on the surface of the graphene nanoplatelets. Fig. 1c and d present low- and high-resolution SEM images of the Ag nanoparticle/graphene nanoplatelet nanocomposite prepared with an Ag loading of 100%, respectively; it is evident that the Ag nanoparticles are uniformly decorated on the surfaces of the graphene nanoplatelets with particle sizes in the range 20−40 nm, as calculated using ImageJ software. The results indicate that the Ag nanoparticle/graphene nanoplatelet nanocomposite can be facilely prepared via a straightforward method with *C. operculatus* leaf extract. SEM images of the Ag nanoparticle/graphene nanoplatelet nanocomposite in Figure S2 show that its morphology was unchanged after storage for three months under ambient conditions, indicating that the Ag nanoparticle/graphene nanoplatelet nanocomposite is highly stable.

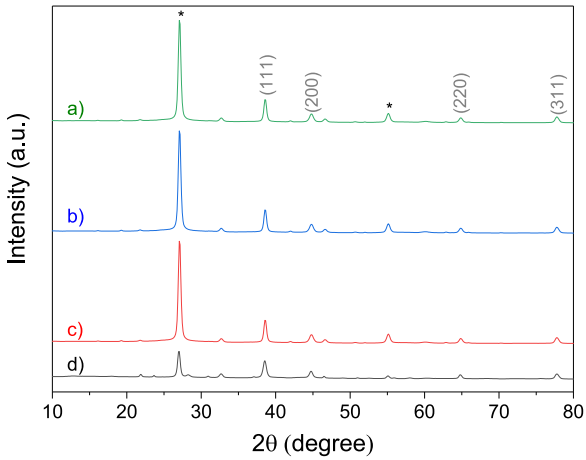

Fig. 2. XRD patterns of the Ag nanoparticle/graphene nanoplatelet nanocomposites prepared with various Ag loading amounts: (a) 30%, (b) 50%, (c) 70% and (d) 100%. * indicates the C in the graphene.

The crystallinity of the Ag nanoparticle/graphene nanoplatelet nanocomposite obtained from various Ag precursor concentrations was investigated via XRD analysis, the results of which are shown in Fig. 2. The XRD patterns confirm the presence of both graphene and Ag nanoparticles in the nanocomposite. While the diffraction peaks at around 2θ values of 26 and 56° indicate carbon in the graphene [40], those at 38.02, 43.58, 64.32 and 77.22° were assigned to the (111), (200), (220) and (311) Brag reflection planes of the face center cubic structure of Ag crystals,

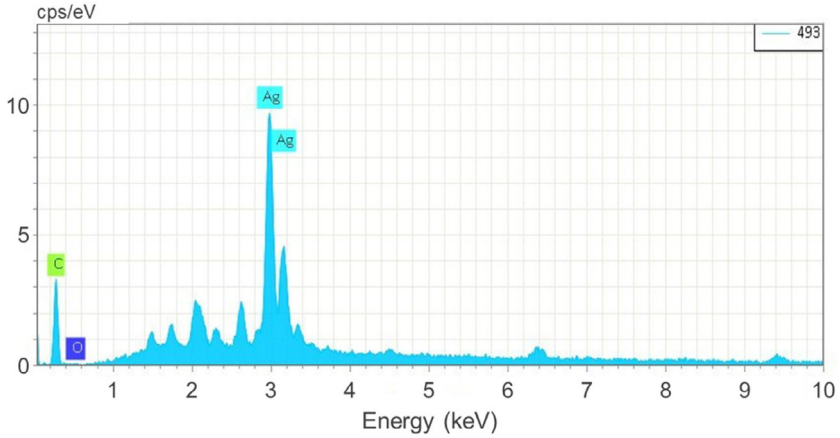

Fig. 3. EDX spectrum for the Ag nanoparticle/graphene nanoplatelet nanocomposite.

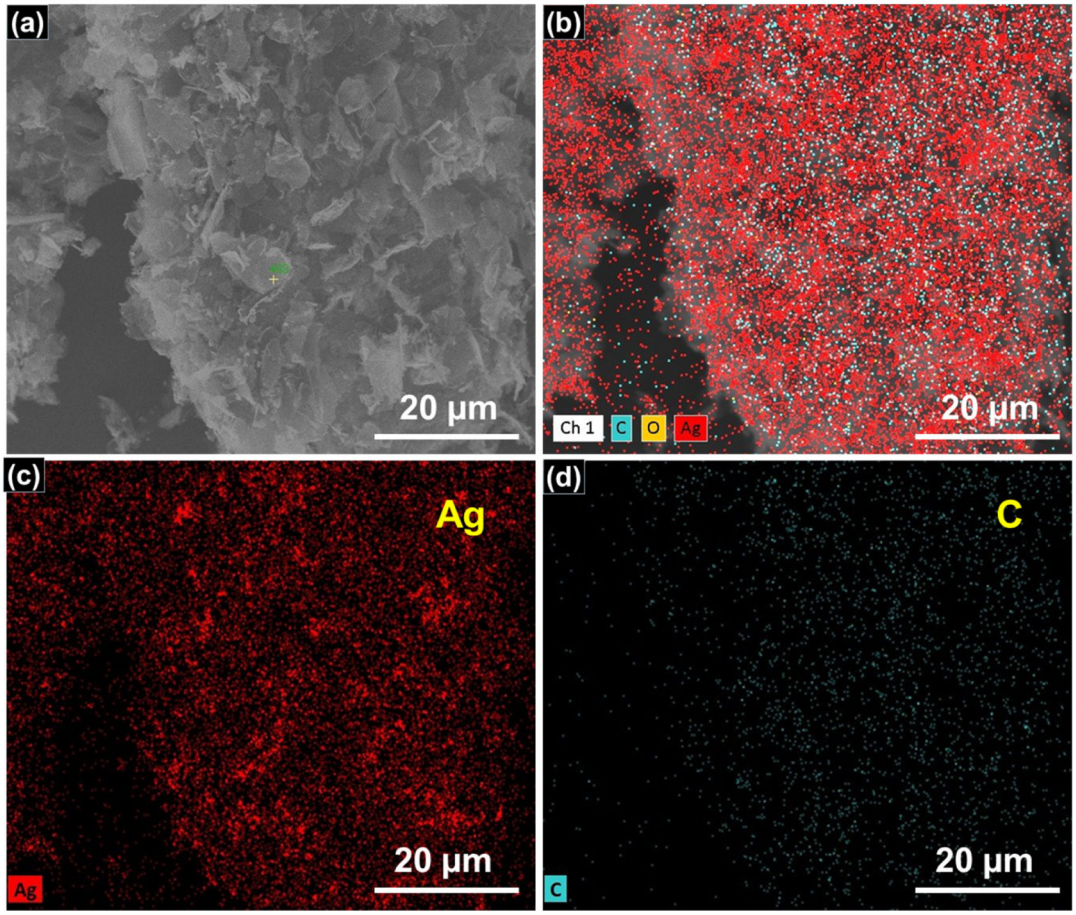

Fig. 4. EDX mapping images of Ag nanoparticle/graphene nanoplatelet nanocomposite.

respectively (JCPDS No. 04-0783) [50,51]. The peak intensity ratio of Ag to C increased according to the increase in Ag loading. At an Ag nanoparticle/graphene nanoplatelet mass ratio of 1:1 (100% Ag), the diffraction peak intensity of Ag was similar to that for the graphene, which indicates that the Ag nanoparticles had almost covered all of the surfaces of the graphene nanoplatelets. Thus, this ratio was optimal for the preparation of the Ag nanoparticle/graphene nanoplatelet nanocomposite for antibacterial applicability. The other small peaks at around 33 and 46.5° were assigned to silver(II) oxide (AgO) (Ag^{2+}) formed on the surface of the Ag crystals [51].

The elemental composition and distributions in the Ag nanoparticle/graphene nanoplatelet nanocomposite were confirmed via EDX analysis and mapping, as shown in Fig. 3. The peaks appearing at around 3 keV indicate the presence of Ag and those at around 0.4 and 0.5 keV indicate C and O, respectively; C was assigned to the graphene, whereas the presence of O could have been due to the oxidation of Ag to Ag_2O and/or from moisture in the environment. However, the percentage of O in the EDX spectrum is negligible, which signifies that the Ag nanoparticle/graphene nanoplatelet nanocomposite obtained from the *C. operculatus* extract is relatively stable. Furthermore, the EDX

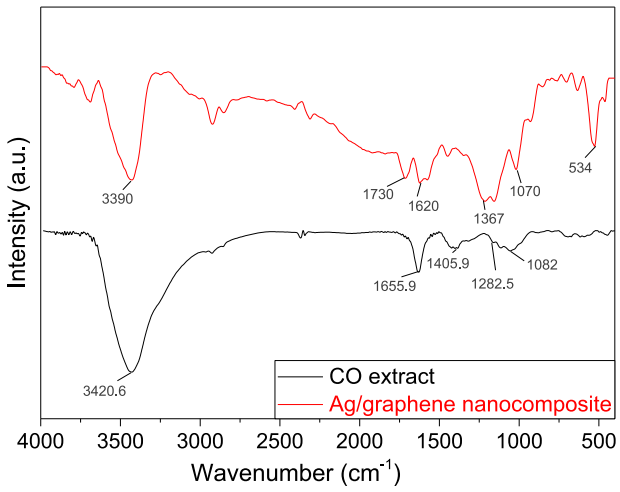

Fig. 5. FTIR spectra of the *C. operculatus* extract and Ag nanoparticle/graphene nanoplatelet nanocomposite prepared from the *C. operculatus* extract.

mapping images in Fig. 4 exhibit Ag nanoparticles uniformly distributed on the surfaces of the graphene nanoplatelets. Once again, the O element is hardly present, thereby indicating that the Ag nanoparticles are protected from oxidation by a functional coating of resins in the *C. operculatus* extract.

FTIR spectroscopy was employed to investigate any functional groups in the *C. operculatus* leaf extract and the Ag nanoparticle/graphene nanoplatelet nanocomposite, as shown in Fig. 5. In the FTIR spectrum of the *C. operculatus* extract, vibration bands at 3420.6, 1655.9, 1405.9, 1282.5 and 1082 cm^{-1} were assigned to the stretching of O-H, C=O, N-H, C-O and C–N bonds, respectively, in the polyphenols, flavonoids, vitamins and resins in the extract. The FTIR spectrum of the Ag nanoparticle/graphene nanoplatelet nanocomposite shows absorption bands for O-H stretching (3390 cm^{-1}), C–C (1620 cm^{-1}), C=O stretching (1730 cm^{-1}), alkoxy C–O stretching (1070 cm^{-1}) and epoxy C–O stretching (1367 cm^{-1}), indicating that the surfaces of the Ag nanoparticles were covered by a thin polysaccharide coating of the resin in the extract, which prevented them from being oxidized. The absorption band intensity at 3390 cm^{-1} declined compared to that in the FTIR spectrum of the *C. operculatus* extract, thereby demonstrating that the O-H groups participated in a redox reaction that reduced Ag^+ to Ag nanoparticles. The stretching vibration of Ag–O bonds was also observed at 534 cm^{-1} [52], thus indicating that the Ag nanoparticles were not only successfully formed on the surfaces of the graphene nanoplatelets but also protected from oxidation by a thin polysaccharide coating from the *C. operculatus* extract. The FTIR spectrum of the free-standing Ag nanoparticles also shows the characteristic vibration band for Ag-O stretching (Figure S3).

Fig. 6 displays the antimicrobial activity results of graphene, Ag nanoparticles and the 1:1 mass ratio Ag nanoparticle/graphene nanoplatelet nanocomposite against *E. coli*. The free-standing graphene shows almost no antibacterial activity (Fig. 6b), whereas inhibition zones of 3, 10 and 16 mm were evident after treatment with 50, 100 and 200 μl of 0.1% Ag nanoparticle/graphene nanoplatelet nanocomposite solution, respectively (Fig. 6c). Interestingly, the Ag nanoparticle/graphene nanoplatelet nanocomposite shows enhanced inhibitory activity against *E. coli* compared to the free-standing Ag nanoparticles (Fig. 6d), with the samples containing 50, 100 and 200 μl of 0.1% Ag nanoparticle/graphene nanoplatelet nanocomposite solution creating inhibited growth zones of 8, 12 and 18 mm in diameter, respectively. The largest inhibition zone of 18 mm with 200 μl of 0.1% Ag nanoparticle/graphene nanoplatelet nanocomposite solution is relatively high and in agreement with the results of Dipankar et al. [53] and Bao et al. [54]. The Ag nanoparticle/graphene nanoplatelet nanocomposite also shows good antimicrobial activity against *Staphylococcus aureus*, *Bacillus subtilis* and *Pseudomonas aerigunosa* (Figure S4). The enhanced antibacterial activity of the Ag nanoparticle/graphene nanoplatelet nanocomposite may be attributed to the uniformly distributed Ag nanoparticles on the surface of the graphene nanoplatelets, enabling more of the former to come into contact with the bacteria, thereby improving the antimicrobial activity.

Table 1
E. coli inhibition zone diameters using the Ag nanoparticle/graphene nanoplatelet nanocomposite as an antimicrobial agent.

Sample	Inhibition zone diameter (mm)		
	50 μl	100 μl	200 μl
Control	0	0	0
Ag nanoparticle/graphene nanoplatelet	8 ± 1.3	12 ± 2	18 ± 2.5

The Ag nanoparticle/graphene nanoplatelet nanocomposite stability was also investigated by storing it at ambient conditions for 30 days, followed by carrying out the same antibacterial experiment against *E. coli*. The results reveal almost the same level of antimicrobial activity as that before storage. This is in good agreement with the SEM images, showing no deterioration of the composite after storage. It can be concluded that the Ag nanoparticle/graphene nanoplatelet nanocomposite exhibits enhanced antimicrobial activity and relative stability because of the protective polysaccharide coating from the *C. operculatus* extract (see Table 1).

4. Conclusions

In summary, an Ag nanoparticle/graphene nanoplatelet nanocomposite was successfully fabricated via a straightforward method using *C. operculatus* leaf extract as a reducing agent to reduce Ag^+ ions to Ag nanoparticles on the surface of graphene nanoplatelets. The polyphenol and flavonoid quantities in the *C. operculatus* extract were determined as 12.4 and 0.62%, which were sufficient to reduce the Ag^+ ions. Ag nanoparticles with a diameter ranging from 20 to 40 nm were uniformly distributed on the surfaces of the graphene nanoplatelets. The Ag nanoparticle/graphene nanoplatelet nanocomposite was stabilized by a protective coating of polysaccharides from the *C. operculatus* extract, which also prevented oxidation of the Ag nanoparticles. The obtained Ag nanoparticle/graphene nanoplatelet nanocomposite exhibited high antimicrobial activity against *E. coli* with a large inhibition growth zone diameter of 18 mm with 200 μl of the 0.1% Ag nanoparticle/graphene nanoplatelet nanocomposite. The Ag nanoparticle/graphene nanoplatelet nanocomposite also showed good antimicrobial activity against *S. aureus*, *B. subtilis* and *P. aerigunosa*. Due to its simple green synthesis and high antimicrobial activity, the Ag nanoparticle/graphene nanoplatelet nanocomposite is a promising material for antibacterial applications. In addition, the *C. operculatus* extract could be employed as an effective reductant for the green synthesis of other nanomaterials.

CRediT authorship contribution statement

Hong Phuong Nguyen Thi: Conceptualization, Writing – original draft. **Kieu Trang Pham Thi:** Methodology, Writing – review & editing. **Le Nguyen Thi:** Data curation, Formal analysis, Writing – review & editing. **Thanh Tung Nguyen:** Data curation, Formal

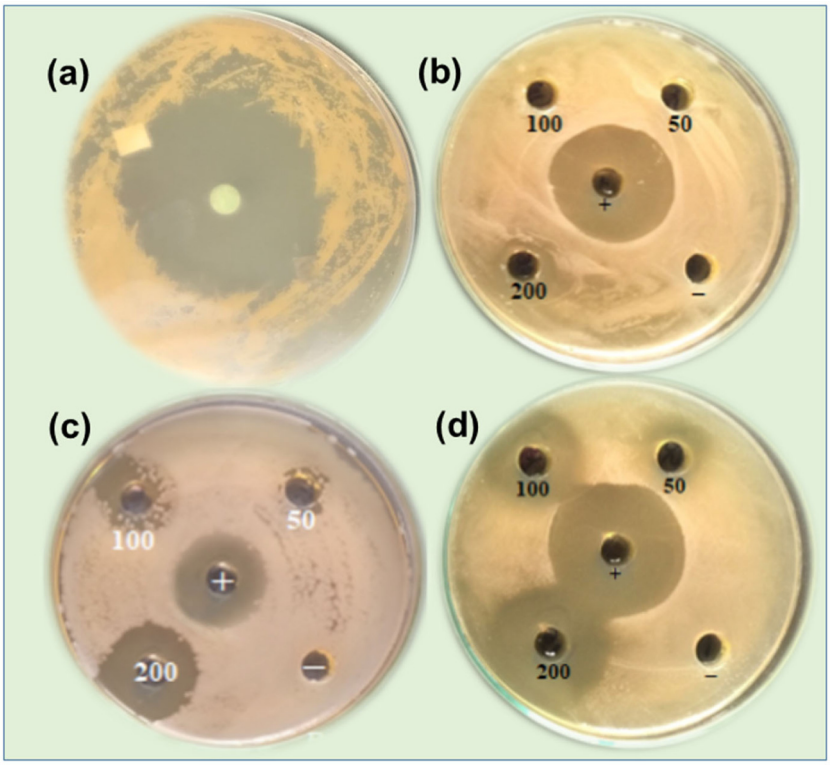

Fig. 6. Antimicrobial activity of (a) the control, (b) graphene, (c) Ag nanoparticles and (d) the 1:1 mass ratio Ag nanoparticle/graphene nanoplatelet nanocomposite against *E. coli* using the agar well diffusion method. (+): positive control (ampicillin); (−): negative control (water).

analysis. **Phuong T.M. Nguyen:** Supervision, Methodology, Data curation, Formal analysis. **Tri Thien Vu:** Methodology, Writing – review & editing. **Hau Thi Le:** Writing – review & editing. **Trung-Dung Dang:** Methodology. **Dang Chinh Huynh:** Writing – review & editing. **Huu Thuan Mai:** Writing – review & editing. **Duc Duong La:** Conceptualization, Supervision, Methodology, Writing – review & editing. **S. Wong Chang:** Writing – review & editing. **D. Duc Nguyen:** Conceptualization, Writing – review & editing.

Declaration of competing interest

The authors declare that they have no known competing financial interests or personal relationships that could have appeared to influence the work reported in this paper.

Acknowledgment

This work is financially funded by the Hanoi Department of Science and Technology (No. 12/2020/HĐ-SKHCN).

Appendix A. Supplementary data

Supplementary material related to this article can be found online at https://doi.org/10.1016/j.nanoso.2021.100810.

References

[1] E.O. Ogunsona, R. Muthuraj, E. Ojogbo, O. Valerio, T.H. Mekonnen, Engineered nanomaterials for antimicrobial applications: A review, Appl. Mater. Today 18 (2020) 100473.
[2] P.T. Nguyen, D.A. Nguyen, T.T. Nguyen, B.T. Le, P.H.T. Nguyen, D.D. La, Low-cost fabrication of Fe_2O_3/rutile nanocomposite from Ilmenite ore: a highly effective adsorbent for removal of arsenic in aqueous media, Adv. Nat. Sci. Nanosci. Nanotechnol. 10 (2019) 015014.
[3] L.A. Kolahalam, I.K. Viswanath, B.S. Diwakar, B. Govindh, V. Reddy, Y. Murthy, Review on nanomaterials: Synthesis and applications, Mater. Today Proc. 18 (2019) 2182–2190.
[4] A.A. Menazea, M.K. Ahmed, Silver and copper oxide nanoparticles-decorated graphene oxide via pulsed laser ablation technique: Preparation, characterization, and photoactivated antibacterial activity, Nano-Struct. Nano-Objects 22 (2020) 100464.
[5] D.D. La, A. Rananaware, H.P.N. Thi, L. Jones, S.V. Bhosale, Fabrication of a TiO_2@ porphyrin nanofiber hybrid material: a highly efficient photocatalyst under simulated sunlight irradiation, Adv. Nat. Sci. Nanosci. Nanotechnol. 8 (2017) 015009.
[6] S. Basak, G. Packirisamy, Nano-based antiviral coatings to combat viral infections, Nano-Struct. Nano-Objects 24 (2020) 100620.
[7] B.D. Deshpande, P.S. Agrawal, M.K.N. Yenkie, S.J. Dhoble, Prospective of nanotechnology in degradation of waste water: A new challenges, Nano-Struct. Nano-Objects 22 (2020) 100442.
[8] S. Ahmed, M. Ahmad, B.L. Swami, S. Ikram, A review on plants extract mediated synthesis of silver nanoparticles for antimicrobial applications: a green expertise, J. Adv. Res. 7 (2016) 17–28.
[9] M. Sui, S. Kunwar, P. Pandey, Q. Zhang, M.-Y. Li, J. Lee, Investigation on the morphology and optical properties of self-assembled ag nanostructures on c-plane GaN by the control of annealing temperature and duration, Nano-Struct. Nano-Objects 15 (2018) 28–39.
[10] D. Garibo, H.A. Borbón-Nuñez, J.N.D. de León, E. García Mendoza, I. Estrada, Y. Toledano-Magaña, H. Tiznado, M. Ovalle-Marroquin, A.G. Soto-Ramos, A. Blanco, J.A. Rodríguez, O.A. Romo, L.A. Chávez-Almazán, A. Susarrey-Arce, Green synthesis of silver nanoparticles using lysiloma acapulcensis exhibit high-antimicrobial activity, Sci. Rep. 10 (2020) 12805.
[11] N. Krithiga, A. Rajalakshmi, A. Jayachitra, Green synthesis of silver nanoparticles using leaf extracts of *Clitoria ternatea* and *Solanum nigrum* and study of its antibacterial effect against common nosocomial pathogens, J. Nanosci. 2015 (2015) 928204.
[12] J.M. Arroyave, M.E. Centurión, J.J. Prías-Barragán, Comparison between electrical and optical properties of Carbon dots, silver nanoparticles and hybrid carbon/silver nanoparticles: Experimental evidence of the interaction of Carbon dots on silver nanoparticles, Nano-Struct. Nano-Objects 24 (2020) 100596.
[13] X. Cai, M. Lin, S. Tan, W. Mai, Y. Zhang, Z. Liang, Z. Lin, X. Zhang, The use of polyethyleneimine-modified reduced graphene oxide as a substrate for silver nanoparticles to produce a material with lower cytotoxicity and long-term antibacterial activity, Carbon 50 (2012) 3407–3415.
[14] P.K. Sethy, P. Mohapatra, S. Patra, D. Bharatiya, S.K. Swain, Antimicrobial and barrier properties of polyacrylic acid/GO hybrid nanocomposites for packaging application, Nano-Struct. Nano-Objects 26 (2021) 100747.

[15] B. Chandu, J. Chittajallu, R.R. Mukkavilli, A.B. Pilli, H.B. Bollikolla, Synthesis and antimicrobial studies of graphene-silver nanocomposite through a highly environmentally benign reduction methodology, Mater. Technol. 33 (2018) 730–736.
[16] L. Zhang, Z. Wang, X. Xu, C. Chen, B. Gao, X. Xiao, Insights into the phosphate adsorption behavior onto 3D self-assembled cellulose/graphene hybrid nanomaterials embedded with bimetallic hydroxides, Sci. Total Environ. 653 (2019) 897–907.
[17] P. Das, S.K. Bhattacharyya, P. Banerji, N.C. Das, Acoustic cavitation assisted synthesis and characterization of photoluminescent carbon quantum dots for biological applications and their future prospective, Nano-Struct. Nano-Objects 25 (2021) 100641.
[18] R. Samiee, B. Ramezanzadeh, M. Mahdavian, E. Alibakhshi, G. Bahlakeh, Graphene oxide nano-sheets loading with praseodymium cations: Adsorption–desorption study, quantum mechanics calculations and dual active-barrier effect for smart coatings fabrication, J. Ind. Eng. Chem. 78 (2019) 143–154.
[19] A.A. Javidparvar, R. Naderi, B. Ramezanzadeh, G. Bahlakeh, Graphene oxide as a pH-sensitive carrier for targeted delivery of eco-friendly corrosion inhibitors in chloride solution: Experimental and theroretical investigations, J. Ind. Eng. Chem. 72 (2019) 196–213.
[20] J.S.C. E, S. Gopi, R. A, S. G, A. Pius, Highly crosslinked 3-D hydrogels based on graphene oxide for enhanced remediation of multi contaminant wastewater, J. Water Process Eng. 31 (2019) 100850.
[21] Y. Kopelevich, P. Esquinazi, Graphene physics in graphite, Adv. Mater. 19 (2007) 4559–4563.
[22] S. Morozov, K. Novoselov, M. Katsnelson, F. Schedin, D. Elias, J. Jaszczak, A. Geim, Giant intrinsic carrier mobilities in graphene and its bilayer, Phys. Rev. Lett. 100 (2008) 016602.
[23] M.A. Ahsan, V. Jabbari, M.T. Islam, R.S. Turley, N. Dominguez, H. Kim, E. Castro, J.A. Hernandez-Viezcas, M.L. Curry, J. Lopez, J.L. Gardea-Torresdey, J.C. Noveron, Sustainable synthesis and remarkable adsorption capacity of MOF/graphene oxide and MOF/CNT based hybrid nanocomposites for the removal of Bisphenol A from water, Sci. Total Environ. 673 (2019) 306–317.
[24] L. De Marchi, C. Pretti, B. Gabriel, P.A.A.P. Marques, R. Freitas, V. Neto, An overview of graphene materials: Properties, applications and toxicity on aquatic environments, Sci. Total Environ. 631–632 (2018) 1440–1456.
[25] D.D. La, S.V. Bhosale, L.A. Jones, N. Revaprasadu, S.V. Bhosale, Fabrication of a Graphene@ TiO_2@ porphyrin hybrid material and its photocatalytic properties under simulated sunlight irradiation, ChemistrySelect 2 (2017) 3329–3333.
[26] P. Kumar, P. Huo, R. Zhang, B. Liu, Antibacterial properties of graphene-based nanomaterials, Nanomaterials 9 (2019) 737.
[27] H. Ji, H. Sun, X. Qu, Antibacterial applications of graphene-based nanomaterials: recent achievements and challenges, Adv. Drug Deliv. Rev. 105 (2016) 176–189.
[28] K. He, Z. Zeng, A. Chen, G. Zeng, R. Xiao, P. Xu, Z. Huang, J. Shi, L. Hu, G. Chen, Advancement of ag–graphene based nanocomposites: an overview of synthesis and its applications, Small 14 (2018) 1800871.
[29] H. Liu, L. Zhong, K. Yun, M. Samal, Synthesis, characterization, and antibacterial properties of silver nanoparticles-graphene and graphene oxide composites, Biotechnol. Bioprocess Eng. 21 (2016) 1–18.
[30] W. Shao, X. Liu, H. Min, G. Dong, Q. Feng, S. Zuo, Preparation, characterization, and antibacterial activity of silver nanoparticle-decorated graphene oxide nanocomposite, ACS Appl. Mater. Interfaces 7 (2015) 6966–6973.
[31] L. Huang, H. Yang, Y. Zhang, W. Xiao, Study on synthesis and antibacterial properties of Ag NPs/GO nanocomposites, J. Nanomater. 2016 (2016).
[32] S. Liu, J. Tian, L. Wang, X. Sun, Microwave-assisted rapid synthesis of Ag nanoparticles/graphene nanosheet composites and their application for hydrogen peroxide detection, J. Nanopart. Res. 13 (2011) 4539–4548.
[33] Z. Çiplak, N. Yildiz, A. Çalimli, Investigation of graphene/ag nanocomposites synthesis parameters for two different synthesis methods, Fuller. Nanotube Carbon Nanostruct. 23 (2015) 361–370.
[34] C. Wen, M. Shao, S. Zhuo, Z. Lin, Z. Kang, Silver/graphene nanocomposite: Thermal decomposition preparation and its catalytic performance, Mater. Chem. Phys. 135 (2012) 780–785.
[35] G. Ding, S. Xie, Y. Liu, L. Wang, F. Xu, Graphene oxide-silver nanocomposite as SERS substrate for dye detection: Effects of silver loading amount and composite dosage, Appl. Surf. Sci. 345 (2015) 310–318.
[36] S. Chen, X. Li, Y. Zhao, L. Chang, J. Qi, Graphene oxide shell-isolated Ag nanoparticles for surface-enhanced Raman scattering, Carbon 81 (2015) 767–772.
[37] S. Rajendrachari, K. BE, Biosynthesis of silver nanoparticles using leaves of Acacia melanoxylon and their application as dopamine and hydrogen peroxide sensors, Phys. Chem. Res. 8 (2020) 1–18.
[38] S. Rajendrachari, B.E.K. Swamy, S. Reddy, D. Chaira, Synthesis of silver nanoparticles and their applications, Anal. Bioanal. Electrochem. 5 (2013) 455–466.
[39] M. Nasrollahzadeh, S. Mahmoudi-Gom Yek, N. Motahharifar, M. Ghafori Gorab, Recent developments in the plant-mediated green synthesis of Ag-based nanoparticles for environmental and catalytic applications, Chem. Rec. 19 (2019) 2436–2479.
[40] M. Tajbakhsh, H. Alinezhad, M. Nasrollahzadeh, T.A. Kamali, Green synthesis of the Ag/HZSM-5 nanocomposite by using Euphorbia heterophylla leaf extract: a recoverable catalyst for reduction of organic dyes, J. Alloys Compd. 685 (2016) 258–265.
[41] M. Nasrollahzadeh, S.M. Sajadi, Preparation of Pd/Fe3O4 nanoparticles by use of Euphorbia stracheyi Boiss root extract: a magnetically recoverable catalyst for one-pot reductive amination of aldehydes at room temperature, J. Colloid Interface Sci. 464 (2016) 147–152.
[42] M. Nasrollahzadeh, M. Sajjadi, J. Dadashi, H. Ghafuri, Pd-based nanoparticles: Plant-assisted biosynthesis, characterization, mechanism, stability, catalytic and antimicrobial activities, Adv. Colloid Interface Sci. 276 (2020) 102103.
[43] A.M. Awwad, N.M. Salem, Green synthesis of silver nanoparticles bymulberry LeavesExtract, Nanosci. Nanotechnol. 2 (2012) 125–128.
[44] H. Bar, D.K. Bhui, G.P. Sahoo, P. Sarkar, S.P. De, A. Misra, Green synthesis of silver nanoparticles using latex of Jatropha curcas, Colloids Surf. A 339 (2009) 134–139.
[45] A. Devadiga, K.V. Shetty, M. Saidutta, Highly stable silver nanoparticles synthesized using Terminalia catappa leaves as antibacterial agent and colorimetric mercury sensor, Mater. Lett. 207 (2017) 66–71.
[46] P. Chettri, V. Vendamani, A. Tripathi, M.K. Singh, A.P. Pathak, A. Tiwari, Green synthesis of silver nanoparticle-reduced graphene oxide using Psidium guajava and its application in SERS for the detection of methylene blue, Appl. Surf. Sci. 406 (2017) 312–318.
[47] N.T.M. Phuong, C. Boger, L. Ulrike, Cytotoxicity and antioxidant activity of plant extracts from Vietnam, Acad. J. Biol. 42 (2020).
[48] V.L. Singleton, J.A. Rossi, Colorimetry of total phenolics with phosphomolybdic-phosphotungstic acid reagents, Am. J. Enol. Vitic. 16 (1965) 144–158.
[49] L. Subedi, S. Timalsena, P. Duwadi, R. Thapa, A. Paudel, K. Parajuli, Antioxidant activity and phenol and flavonoid contents of eight medicinal plants from Western Nepal, J. Trad. Chin. Med. 34 (2014) 584–590.
[50] B. Genorio, W. Lu, A.M. Dimiev, Y. Zhu, A.-R.O. Raji, B. Novosel, L.B. Alemany, J.M. Tour, In situ intercalation replacement and selective functionalization of graphene nanoribbon stacks, ACS Nano 6 (2012) 4231–4240.
[51] M.D.D. La, S. Bhargava, S.V. Bhosale, Improved and a simple approach for mass production of graphene nanoplatelets material, ChemistrySelect 1 (2016) 949–952.
[52] P.P. Dutta, M. Bordoloi, K. Gogoi, S. Roy, B. Narzary, D.R. Bhattacharyya, P.K. Mohapatra, B. Mazumder, Antimalarial silver and gold nanoparticles: Green synthesis, characterization and in vitro study, Biomed. Pharmacother. 91 (2017) 567–580.
[53] J. Ma, J. Zhang, Z. Xiong, Y. Yong, X. Zhao, Preparation, characterization and antibacterial properties of silver-modified graphene oxide, J. Mater. Chem. 21 (2011) 3350–3352.
[54] A.A. Alawfi, F.Z. Henari, A. Younis, H. Manaa, Bio-inspired synthesis of silver nanoparticles using Hibiscus Tiliaceus L. flower extracts for improved optical characteristics, J. Mater. Sci. Mater. Electron. 31 (2020) 21073–21081.